



The dynamics of supraglacial ponds in the Everest region, central Himalaya

C. Scott Watson^{*}, Duncan J. Quincey, Jonathan L. Carrivick, Mark W. Smith

School of Geography and water@leeds, University of Leeds, Leeds LS2 9JT, UK



ARTICLE INFO

Article history:

Received 28 January 2016

Received in revised form 4 April 2016

Accepted 25 April 2016

Available online 27 April 2016

ABSTRACT

The dynamics of supraglacial pond development in the Everest region are not well constrained at a glacier scale, despite their known importance for meltwater storage, promoting ablation, and transmitting thermal energy englacially during drainage events. Here, we use fine-resolution (~0.5–2 m) satellite imagery to reveal the spatiotemporal dynamics of 9340 supraglacial ponds across nine glaciers in the Everest region, ~2000–2015. Six of our nine study glaciers displayed a net increase in ponded area over their observation periods. However, large inter- and intra-annual changes in ponded area were observed of up to 17% (Khumbu Glacier), and 52% (Ama Dablam) respectively. Additionally, two of the fastest expanding lakes (Spillway and Rongbuk) partially drained over our study period. The Khumbu Glacier is developing a chain of connected ponds in the lower ablation area, which is indicative of a trajectory towards large lake development. We show that use of medium-resolution imagery (e.g. 30 m Landsat) is likely to lead to large classification omissions of supraglacial ponds, on the order of 15–88% of ponded area, and 77–99% of the total number of ponds. Fine-resolution imagery is therefore required if the full spectrum of ponds that exist on the surface of debris-covered glaciers are to be analysed.

© 2016 Elsevier B.V. All rights reserved.

1. Introduction

The increased storage of meltwater in supraglacial, proglacial and ice-marginal settings is symptomatic of deglaciation and is a globally observed trend (Carrivick and Tweed, 2013). Glacial lake development across the central Himalaya (India, Nepal, Bhutan, Tibet (China)) (e.g. Komori, 2008; Gardelle et al., 2011; Nie et al., 2013; Veettil et al., 2015; Wang et al., 2015; Zhang et al., 2015) corresponds with warming temperatures and a trend of negative glacier mass balance (Kääb et al., 2012). The negative mass balance is well known to be modulated by the variable thickness of debris cover that promotes glacier surface lowering in conjunction with a relatively stable terminus position (Bolch et al., 2011). These mass balance trends and glacier characteristics are well documented in the Everest region (e.g. Bolch et al., 2008a, 2011; Benn et al., 2012; Ye et al., 2015), where surface lowering and increasing glacier stagnation has been highlighted to promote increased supraglacial pond formation and their potential coalescence into larger lakes where a low glacier surface gradient exists (Watanabe et al., 1994; Richardson and Reynolds, 2000; Quincey et al., 2007; Rohl, 2008; Thompson et al., 2012).

Glacier-scale observations of the links between areas of high downwasting and the location of ice cliffs and ponds, further reveal their importance for debris-covered glacier ablation (e.g. Immerzeel et al., 2014; Pellicciotti et al., 2015). Local-scale measurements and

modelling of ice cliff retreat (e.g. Reid and Brock, 2014; Steiner et al., 2015) and pond energy balance (e.g. Sakai et al., 2000; Miles et al., 2016) have greatly improved process-based understanding in recent years. These ponds also play an important part in the glacier ablation budget, through the transmission of thermal energy to subaqueous ice and to adjacent ice cliffs (Sakai et al., 2000; Benn et al., 2001; Rohl, 2006; Miles et al., 2016). It may be hypothesised that ponds dynamics will be associated with patterns of glacier surface lowering and ice cliff calving. However, this hypothesis remains to be tested because quantitative measurements have hitherto been spatially limited to individual pond basins (e.g. Benn et al., 2001).

Studies focusing specifically on surface water storage in the Everest region have been regionally aggregated (e.g. Gardelle et al., 2011), glacier or lake specific (e.g. Bolch et al., 2008b; Thompson et al., 2012), or covering one point in time (e.g. Salerno et al., 2012) (Table 1). Whilst these approaches are merited, they are often limited by data availability, which has historically tended towards coarser-resolution imagery, and data suitability, which cannot be determined without ground-truth or fine-resolution imagery. In the Everest region and across the Himalaya previous studies have generally utilised 30 m resolution multi-spectral Landsat imagery, owing to the large temporal archive and simple band ratio application to delineate water bodies (e.g. Gardelle et al., 2011; Nie et al., 2013; Bhardwaj et al., 2015; Liu et al., 2015; Wang et al., 2015). ASTER (Advanced Spaceborne Thermal Emission and Reflection Radiometer) imagery (15 m resolution) is also popular for glacier-scale applications (e.g. Wessels et al., 2002; Bolch et al., 2008b; Thompson et al., 2012), although the archive is shorter (2000–present

^{*} Corresponding author.

E-mail address: scott@rockyglaciers.co.uk (C.S. Watson).

Table 1
Remote sensing studies of supraglacial water storage in the Everest region.

Reference	Date range	Coverage overlap with this study	Imagery (resolution)	Notes
Iwata et al. (2000)	1978–1995	Khumbu Glacier	SPOT (not specified)	A sketch map made with SPOT imagery was compared to that of a field survey in 1978
Wessels et al. (2002)	2000	Ngozumpa, Khumbu and Rongbuk glaciers	ASTER (15 m)	Band ratios were used to delineate water for a single time period. Turbid lakes were found in hydrologically connected regions
Bolch et al. (2008b)	1962–2005	Khumbu, Lhotse and Imja glaciers	Corona, Landsat, topographic maps, Ikonos, ASTER (2–79 m)	Normalised Difference Water Index (NDWI) and/or manual delineation was used to classify water bodies.
Gardelle et al. (2011)	1990–2009	All glaciers	Landsat (30 m)	A decision tree was used to classify lakes incorporating the NDWI. A minimum lake size of 3600 m ² was used. Area change was not reported for individual glaciers, other than a brief comparison with Bolch et al. (2008b). An association between negative mass balance and lake expansion is presented
Salerno et al. (2012)	2008	All except Rongbuk Glacier	AVNIR-2 (10 m)	Water bodies were manually digitised for a single time period
Thompson et al. (2012)	1984–2010	Ngozumpa Glacier	Aerial photographs (<1 m), ASTER (15 m)	A multi-temporal analysis of the expansion of Spillway Lake was conducted using satellite imagery and field surveys
Nie et al. (2013)	1990–2010	All glaciers	Landsat (30 m)	OBIA was combined with NDWI-based water detection. Pondered area change was not reported for individual glaciers.
Zhang et al. (2015)	1990–2010	All glaciers	Landsat (30 m)	Water bodies were manually digitised with a minimum lake size threshold of 2700 m ² . Pondered area change was not reported for individual glaciers.

Note: studies reporting the expansion of Imja Lake are not included.

day). Both sensors are limited by their spatial resolution, meaning associated studies have not been able to focus on detailed changes in ponds through time. This paper aims to present the first fine-resolution spatio-temporal analysis of supraglacial pond dynamics to address this shortcoming. We analyse Google Earth, Quickbird, GeoEye and WorldView imagery (0.7–2 m) covering nine glaciers in the Everest region of the central Himalaya. Our objectives are to: (1) characterise the spatial evolution of supraglacial ponds on an individual glacier scale; (2) quantify short-term seasonal and inter-annual change in supraglacial pond area in the region; and (3) evaluate the implications of using medium-resolution satellite imagery (e.g. 15–30 m) to delineate the full spectrum of pond sizes that exist on Himalayan debris-covered glaciers.

2. Study region

Annual precipitation in the Everest region is dominated by the Indian summer monsoon and the majority of rainfall (~80%) occurs between June–September (Bookhagen and Burbank, 2006; Wagnon et al., 2013). Both the northerly draining Rongbuk catchment and the southerly draining Dudh Koshi catchment display a trend of warming temperatures (Yang et al., 2006; Shrestha and Aryal, 2011), which in conjunction with a potentially delayed (Mölg et al., 2012) and/or weakening monsoon will reduce glacier accumulation (Salerno et al., 2015). Decreasing monsoonal precipitation is likely implicated in reduced glacier driving stresses, causing terminus stagnation and the subsequent development of supraglacial ponds and lakes in the region (Quincey et al., 2009; Salerno et al., 2015). The decadal response of large debris-covered glaciers to climate change suggests negative mass balance conditions will prevail in coming decades, irrespective of any slowdown to contemporary warming (Rowan et al., 2015).

The Everest region is characterised by glaciers that are heavily debris-covered in their lower reach (Fig. 1). The debris is sourced from rock fall avalanches and from moraine ridge collapses, and typically increases in thickness towards glacier termini (Nakawo et al., 1986). The glaciers are low gradient in the debris-covered area (Quincey et al., 2007), stagnating (Quincey et al., 2009; Dehecq et al., 2015), and are widely losing mass (Bolch et al., 2008a, 2011; Ye et al., 2015). Supraglacial ponds are prevalent features on the low gradient and hummocky topography of debris-covered glacier ablation zones. They vary in size, shape and turbidity (Fig. 2) as well as situation; some are surrounded by large, calving ice-cliffs whereas others sit in debris-lined hollows. The distinction between what may be described as a

pond vs a lake is not well-defined (either theoretically or physically) so herein we refer to all surface water as ponds, unless specifically named otherwise (e.g. Spillway Lake on the Ngozumpa Glacier). Regardless of their size, the upper surface freezes over during the winter period (December–February), although a partially frozen surface may be present up to several months earlier.

Nine debris-covered glaciers in the Everest region spanning Nepal (8) and Tibet (1) were selected for supraglacial pond analysis (Fig. 1). These nine glaciers drain the Dudh Koshi and Rongbuk catchments respectively. The Rongbuk, Ngozumpa, and Khumbu glaciers are the longest in the study area with debris-covered lengths of ~15 km, ~11 km, and ~11 km, respectively; the shortest is Imja Glacier at ~2 km. The glaciers predominantly flow in a southerly direction with the exceptions of Rongbuk and Ama Dablam Glaciers (northerly flowing), and Imja Glacier (westerly flowing).

3. Data sources

This study used 16 time periods of fine-resolution imagery (Table 2), comprising nine from Google Earth (<2 m spatial resolution), and seven from WorldView 1 & 2, GeoEye, and QuickBird 2 sensors (0.5–0.6 m spatial resolution). This imagery incorporated post-monsoon/winter periods (termed winter herein) (late September–February), and pre-monsoon/monsoonal periods (termed summer herein) (March–mid September). True-colour orthorectified Google Earth images were accessed using Google Earth Pro. WorldView, GeoEye and Quickbird scenes were orthorectified in ERDAS Imagine using rational polynomial coefficients and the 30 m Shuttle Radar Topography Mission (SRTM) Digital Elevation Model (DEM). Glacier outlines were obtained from the South Asia – East Randolph Glacier Inventory 5.0 (Pfeffer et al., 2014). These outlines were modified manually to reflect the debris-covered area of each study glacier, and only supraglacial ponds falling within this masked area were included in the study.

4. Methods

4.1. Supraglacial pond classification

A total of 9340 ponds were classified in this study either semi-automatically using an object-based classification (46%), or manually digitised in Google Earth (54%).

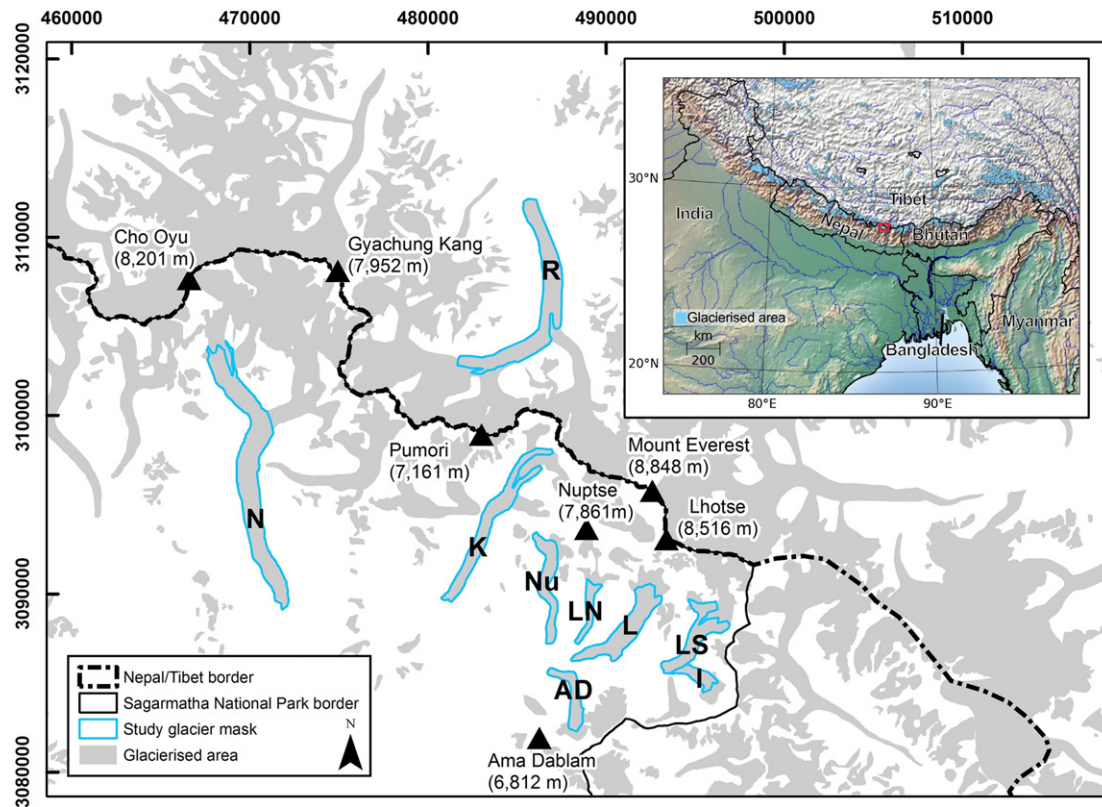


Fig. 1. Location of the nine study glaciers within the central Himalaya (inset). Selected mountain peaks are shown. K – Khumbu Glacier, N – Ngozumpa Glacier, R – Rongbuk Glacier, Nu – Nuptse Glacier, LN – Lhotse Nup Glacier, L – Lhotse Glacier, LS – Lhotse Shar Glacier, I – Imja Glacier, AD – Ama Dablam Glacier.

4.1.1. Object based image analysis (OBIA)

For satellite image classifications OBIA offers several advantages over pixel-based approaches. First, it has the ability to detect edges at multiple scales, providing a set of connected curves delineating the boundaries of surface ponds (and other spectrally discontinuous features) regardless of their size. Secondly, in doing this, OBIA also makes use of non-spectral metrics (e.g. image texture) to classify segments, which generally leads to a more refined output than can be achieved using pixel-based approaches. Thirdly, because OBIA leads to the derivation of homogeneous polygons, there is minimal noise in the segmented image, in contrast to often-used ratios such as the Normalised Difference Water Index (Liu et al., 2015). In a Himalayan context, OBIA has previously been applied to Landsat imagery for glacial lake detection (e.g. Nie et al., 2013; Liu et al., 2015) and glacier extent mapping (Nie et al., 2010). We applied it to the panchromatic band of each WorldView, GeoEye, and QuickBird image using ENVI 5.2, to effectively delineate the edges of supraglacial ponds (Fig. 3). For this analysis the original panchromatic images were resampled to a common resolution of 0.7 m.

Errors in the OBIA approach can arise from under- or over-segmentation of the image, which is sensitive to image-specific scale and merge thresholds. For an under-segmented image, pond boundaries contain adjacent terrain, which cannot be retrospectively removed without manual boundary editing, whereas an over-segmented image represents individual objects with several or more polygons, which can be merged manually (Liu and Xia, 2010). We opted to over-segment each image and then manually inspect each classified pond, editing and merging polygons where required. Segmentation in ENVI involved scale and merge thresholds of ~15 to 25 and ~70 to 80 respectively. Manual merging was generally only necessary where a pond featured partial coverage of floating ice. Pond boundaries were spectrally

distinct from the surrounding debris-cover so misclassification was minimal (Fig. 3). Multi-spectral imagery was available for most time periods (Table 2) and was cross-referenced with the panchromatic imagery to check pond boundaries. The final pond boundaries were exported to ArcGIS for analysis. This methodology was chosen to avoid the reliance on user-defined thresholds and hence provide the highest possible classification accuracies, rather than develop a semi-automatic classification technique.

4.1.2. Manual digitisation

Eight periods of Google Earth imagery (<2 m spatial resolution) increased the temporal resolution and spread of our dataset (Table 2). A supplementary ninth image, which did not have full coverage of the Ngozumpa Glacier, was used to quantify the size of Spillway Lake in Jun-15. As we were unable to use the OBIA approach on the Google Earth imagery we digitised the surface ponds by hand in Google Earth Pro and imported the polygons into ArcGIS for further analysis. All digitisation was undertaken by one operator to ensure consistency and ponds in each image were checked for accuracy by revisiting on independent days until no further edits were required.

4.1.3. Uncertainty

Differential GPS (dGPS) points were taken on the boundaries of four stable ponds on the Khumbu Glacier in Oct/Nov 2015 to check against our most recent pond inventory (February 2015). The ponds were clear, on a stagnant and vegetated zone of the glacier (Inoue, 1980; Quincey et al., 2009), and were observed to be stable over our study period. dGPS points showed good agreement with classified pond boundaries and generally fell on or within a one pixel margin of the boundary (Supplementary Fig. 1).

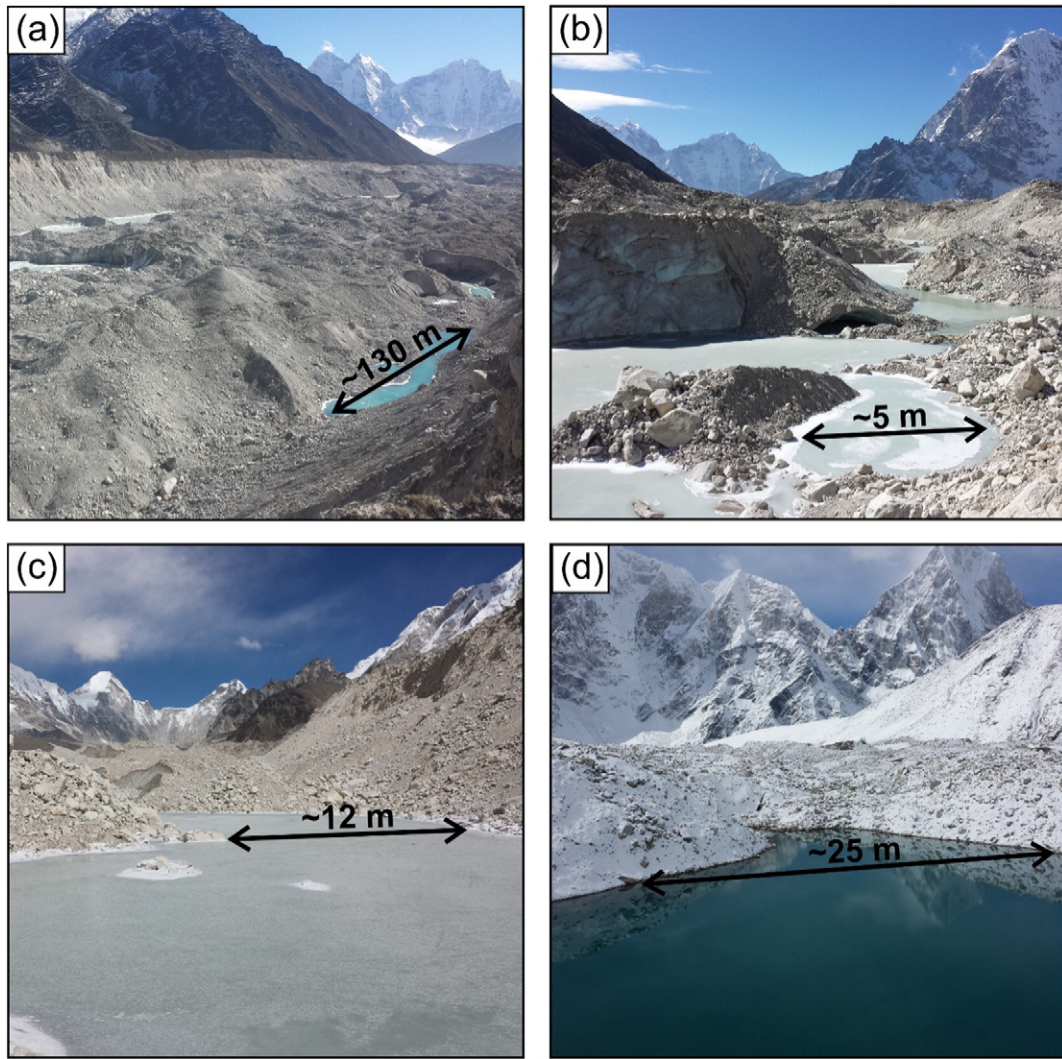


Fig. 2. Examples of the sizes, shapes, and sediment concentrations of supraglacial ponds on the Khumbu Glacier. Approximate scales are shown for individual ponds. (a) Looking south over across a turbid elongated pond, (b) a turbid and partially frozen irregular shaped pond with adjacent ice cliffs, (c) a completely frozen pond with a more regular shoreline, and (d) a clear and stable pond with a smooth shoreline.

Table 2
Spatial and temporal coverage of imagery used in this study.

Image ID/description and spatial resolution	Image date	K	N	R	Nu	LN	L	LS	I	AD
Google Earth. Supplementary image with Spillway Lake coverage. MS.	07/06/2015		**							
103001003D7AFE00/WV02 sensor. PMS. 0.52–2.11	02/02/2015	*		*						
Google Earth. MS	24/01/2015					*	*	*	*	
Google Earth. MS	13/01/2014	*			*					*
Google Earth. MS	08/12/2013					*	*	*	*	
ArcGIS Basemap.	10/07/2013	**								
WV02. MS. 0.50 m										
Google Earth. MS	23/05/2013					*				
1050410000E0AE00/GE01. P. 0.50 m	23/12/2012		*							
103001001C5E7600/WV02. PMS. 0.51–2.05 m	11/10/2012			*						
101001000E521A00/QB02. PMS. 0.67–2.67 m	19/10/2011	*		*	*	*	*	*	*	*
102001001745CD00/WV01. P. 0.52 m	17/10/2011		*							
Google Earth. MS	09/06/2010		**							
Google Earth. MS	03/11/2009	*	*							*
Google Earth. MS	24/05/2009	**								**
10100100013F4E00/QB02. PMS. 0.62–2.49 m	20/09/2002				*	*	*	*		
Google Earth. MS	18/12/2000									*

WV = WorldView, GE = GeoEye, and QB = QuickBird sensors. MS = multi spectral, P = panchromatic, PMS = panchromatic and multi spectral. Spatial resolution (panchromatic – multi spectral).

Image date ddmmyyyy. “*” & “**” indicate glacier coverage for non-monsoonal (winter), and pre-monsoon/monsoonal images (summer) respectively.

K – Khumbu Glacier, N – Ngozumpa Glacier, R – Rongbuk Glacier, Nu – Nuptse Glacier, LN – Lhotse Nup Glacier, L – Lhotse Glacier, LS – Lhotse Shar Glacier, I – Imja Glacier, AD – Ama Dablam Glacier.

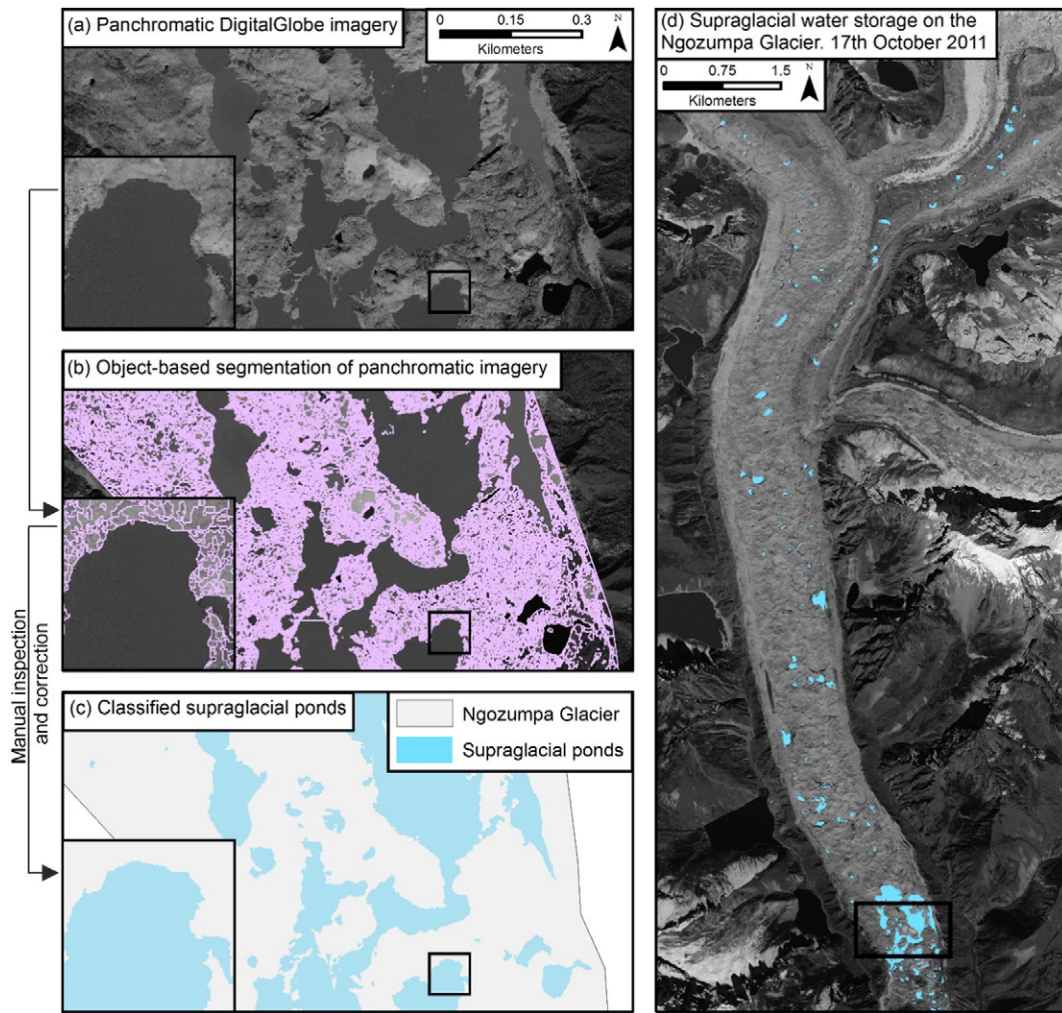


Fig. 3. The workflow of using panchromatic DigitalGlobe imagery to classify supraglacial ponds. (a) A subset of the original WorldView 1 panchromatic band, (b) object-based edge segmentation on the panchromatic band to delineate surface water, (c) classified supraglacial pond output following manual inspection and correction, and (d) supraglacial ponds on the Ngozumpa glacier (11th Oct 2011).

Satellite image courtesy of the DigitalGlobe Foundation.

Uncertainty in classified ponded area was calculated by assuming ± 1 pixel in the perimeter of each pond following Gardelle et al. (2011). Although pixel resolution is not explicitly stated in Google Earth imagery, we assumed it to be 1 m for uncertainty estimation based on our field observations compared to the size of features that could be discriminated in the imagery.

In order to assess the uncertainty of the OBIA outputs relative to manual digitisation, one operator manually digitised 50 additional ponds on a panchromatic (0.7 m resolution) image (Supplementary Table 1). The areas of digitised polygons were compared to OBIA derived polygons and the area uncertainty when using a ± 1 pixel boundary (i.e. the uncertainty assumed in this study). The area difference between OBIA and manual classification methods ranged from 0.3 to 16% with a mean of 6%, whereas the assumed uncertainty using a ± 1 pixel buffer ranged from 6 to 69% with a mean of 25%. Therefore the uncertainty bounds used in our study are well above the actual uncertainty expected during pond classification.

4.2. Pond and glacier characteristics

Ponded area change with distance up-glacier was calculated using 500 m distance bins from the terminus of each glacier, accounting for curvature along a centreline. Mean pond circularity was calculated

using Eq. (1), since some studies have assumed circular ponds when assessing theoretical error (e.g. Salerno et al., 2012).

$$\text{Circularity} = \left(\frac{P^2}{4\pi A} \right) \quad (1)$$

where P and A are pond perimeter (m) and area (m^2) respectively.

The transition between active and inactive ice was approximated for each glacier using the velocity map outputs of Bolch et al. (2008b); Quincey et al. (2009); Haritashya et al. (2015), and Dehecq et al. (2015), unless this transition occurred up-glacier of the study mask.

4.2.1. Pond area bins

The areas of individual ponds were classified into 300 m^2 bins and used to derive cumulative area distributions for each glacier. 300 m^2 bins were chosen to allow scaling to reflect the Landsat pixel size and were used to estimate potential area uncertainties when using coarser-resolution imagery.

4.2.2. Pond frequency

Pond frequency was derived by summing pond area pixels in each image and then normalising the score to derive percentage occurrence over respective images. Pond frequency reveals areas of likely continual

pond development, in contrast to areas where ponds were ephemeral. An important distinction exists between ponds that persist over two or more images, those that drain, and those that drain and subsequently refill between time periods. However, the imagery used in this study is of insufficient temporal resolution to report such trends reliably, which would ideally require field-based observations. Additionally, a pond-scale analysis was not the aim of this study. For this reason we take pond frequency to represent a pixel that was classified as water for one or more time periods.

5. Results

5.1. Study region ponded area change

Overall change in ponded area across the study glaciers displayed a heterogeneous spatial pattern (Fig. 4). Considering the largest glaciers (Ngozumpa, Rongbuk, and Khumbu) without their respective terminus lakes, the Ngozumpa Glacier displayed a net loss in ponded area of 29,864 m² (Nov-09–Dec-12), the Rongbuk Glacier gained 1664 m² (Oct-11–Feb-15), and the Khumbu Glacier gained 99,889 m² (Nov-09–Feb-15). The smaller study glaciers (Nuptse, Lhotse Nup, Lhotse, Lhotse Shar, and Imja) all featured a ponded area minimum in Oct-11, followed by an increase in surface water storage thereafter. Our analysis showed that without exception there were more ponds evident during summer periods than during the preceding winter (and an according increase in ponded area) (Table 3, Fig. 4). An exceptional increase in ponded area was observed on Khumbu and Ama Dablam glaciers in May-09.

The large supraglacial lakes on the termini of the Ngozumpa and Rongbuk glaciers, termed Spillway Lake and Rongbuk Lake respectively, were both dynamic over the study period (Fig. 4, Table 3) but did not reflect historic trends of expansion (Ye et al., 2009; Thompson et al., 2012). The area of Rongbuk Lake consistently declined (losing 87,451 m², Oct-11–Feb-15), whereas Spillway Lake expanded over the period Nov-09 to Jun-10, but displayed an overall net loss 34,566 m² (Nov-09–Dec-12). The supplementary Google Earth image from Jun-15 revealed contemporary expansion of Spillway Lake by 26,221 m² from Dec-12, reducing the net loss to 8345 m² (Nov-09–Jun-15). The size of Spillway Lake and adjacent ponds was 272,982 m² in Nov-09. This is in agreement with the value of ~258,000 m² (December 2009) reported by Thompson et al. (2012) from a dGPS survey of the lake edge, which also included several additional smaller ponds.

5.2. Spatial characteristics

5.2.1. Glacier-scale pond dynamics

We divided our dataset into the three large glaciers (Fig. 5a), and the six smaller glaciers (Fig. 5b) to evaluate ponded area trends up-glacier. Fig. 5 reveals areas of pond drainage, growth, or stability. As these trends are reported across distance bins they do not reveal individual pond dynamics, but instead highlight areas of dynamic pond activity.

For the large glaciers (Fig. 5a), areas of greatest pond area often persisted through each image, whilst the magnitude of the total area changed. The relationship between ponded area and distance from the terminus is thus non-monotonic and displays regular variation. This relationship is most pronounced for the Khumbu Glacier, with peaks in ponded area approximately every 2 km moving up-glacier. Ponded

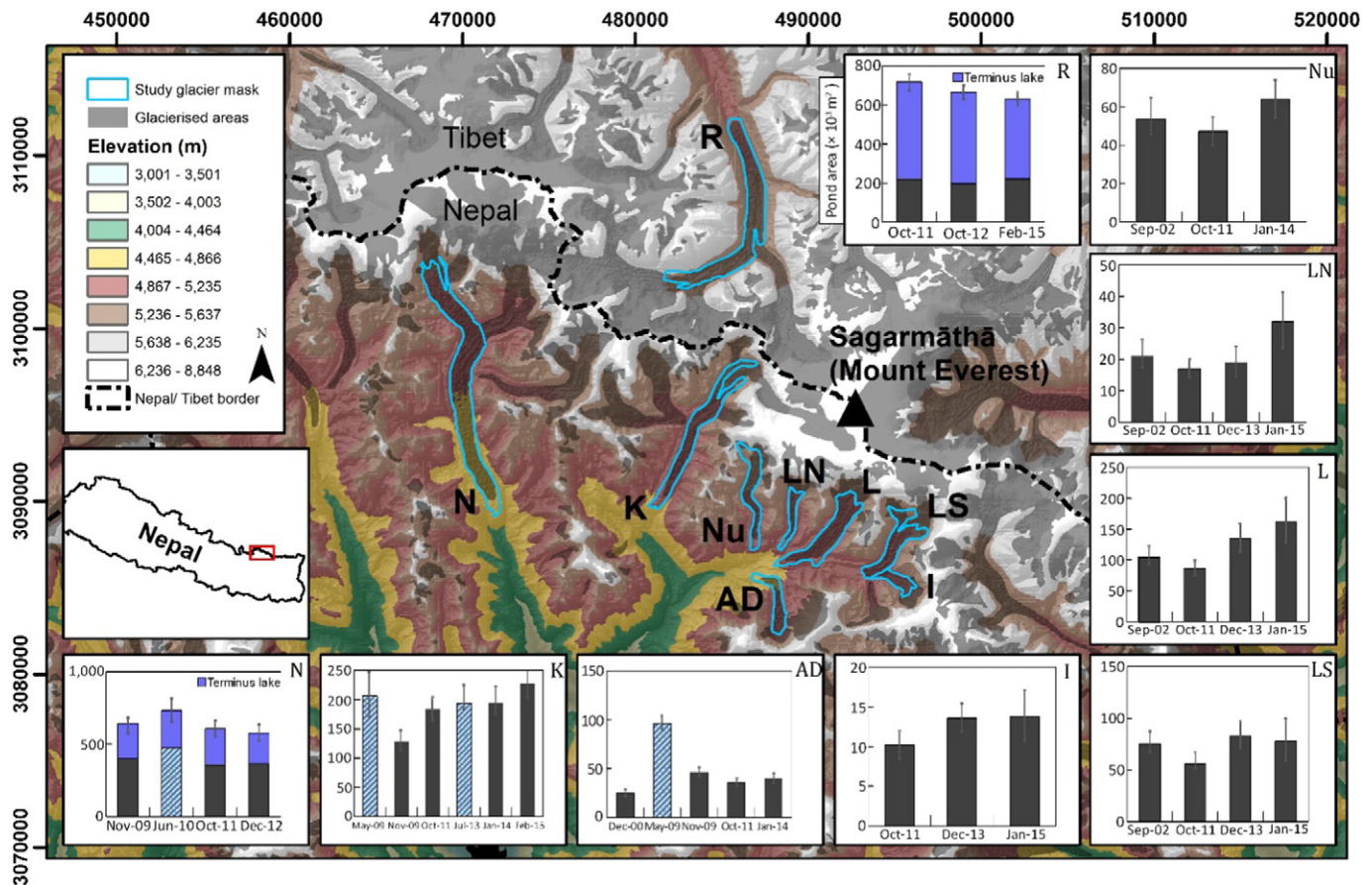


Fig. 4. Overall supraglacial water storage change within the masked study glacier areas. Error bars are derived from a ± 1 pixel uncertainty for classified ponds. Capped purple bars for the Rongbuk and Ngozumpa glaciers represent the area changes of Rongbuk and Spillway lakes respectively. Hashed blue columns represent summer images. K – Khumbu Glacier, N – Ngozumpa Glacier, R – Rongbuk Glacier, Nu – Nuptse Glacier, LN – Lhotse Nup Glacier, L – Lhotse Glacier, LS – Lhotse Shar Glacier, I – Imja Glacier, AD – Ama Dablam Glacier.

Table 3
Supraglacial pond inventory characteristics and area change.

Glacier ID	Debris-covered area (km ²)	Image date (dd/mm/yyyy)	Supraglacial ponds		
			Number	Area (m ²)	Mean circularity ^a
K	7.1	02/02/2015	362	228,391	3.6
		13/01/2014	285	183,723	1.7
		10/07/2013	301	193,562	2.0
		19/10/2011	259	183,980	3.4
		03/11/2009	185	12,502	1.8
		24/05/2009	471	206,590	2.9
N	16.3	07/06/2015		^b 272,982	
		23/12/2012	770	579,152	3.0
				^b 246,761	
		17/10/2011	563	607,356	3.5
				^b 289,671	
		09/06/2010	1022	733,641	1.6
R	11.4	03/11/2009	545	^b 300,602	
				643,582	1.7
				^b 281,327	
		02/02/2015	333	632,019	3.4
				^b 409,659	
		11/10/2012	352	665,805	2.8
Nu	3.9			^b 469,186	
		19/10/2011	420	717,806	3.0
				^b 497,110	
		13/01/2014	131	63,788	1.5
		19/10/2011	163	47,080	2.6
		20/09/2002	132	53,332	3.1
LN	1.5	24/01/2015	145	32,392	2.0
		08/12/2013	77	18,812	1.7
		19/10/2011	63	16,760	2.6
		20/09/2002	66	21,271	2.8
		24/01/2015	722	161,709	1.8
		08/12/2013	344	134,564	1.6
L	6.3	19/10/2011	211	86,699	2.7
		20/09/2002	207	105,192	2.7
		24/01/2015	355	78,397	1.8
		08/12/2013	174	82,748	1.8
		19/10/2011	144	56,297	2.5
		20/09/2002	164	74,899	2.7
LS	4.7	24/01/2015	52	13,767	1.9
		08/12/2013	25	13,585	1.6
		19/10/2011	39	10,186	2.9
		13/01/2014	52	40,124	1.6
		19/10/2011	53	35,607	2.8
		03/11/2009	39	46,171	1.6
I	1.5	24/05/2009	76	96,547	1.5
		18/12/2000	38	24,517	1.4

K – Khumbu Glacier, N – Ngozumpa Glacier, R – Rongbuk Glacier, Nu – Nuptse Glacier, LN – Lhotse Nup Glacier, L – Lhotse Glacier, LS – Lhotse Shar Glacier, I – Imja Glacier, AD – Ama Dablam Glacier.

^a A circle would have a score of 1. Examples are given in Supplementary Fig. 1.

^b Contributing area of terminal lakes (Ngozumpa Glacier: Spillway Lake; Rongbuk Glacier: Rongbuk Lake).

area on the Khumbu increased over much of the glacier through time, but especially in the lower 7 km. Relative to winter images (grey scale), summer images (blue scale) featured increased ponded area through time in the upper 6 km of the Khumbu, in contrast to a decreased area near the terminus (0.5–4 km), although only two summer time periods were available for comparison (Fig. 5a).

Spillway and Rongbuk lakes migrated up-glacier over the observation period and their overall size diminished (Fig. 5a, Table 3). Up-glacier expansion of Spillway Lake (Fig. 6b) was coincident with locations of ice cliffs and lake deepening identified by Thompson et al. (2012, cf. their Fig. 6c). Pond variability was low immediately up-glacier of both lakes, although this variability extended notably further on the Rongbuk Glacier before reaching an increase in ponded area at ~8.0 km (Fig. 5a).

Surface water storage on the smaller glaciers in the region (Fig. 5b) was much more variable. In recent years the greatest expansion in ponded area was in the regions of 2.5 to 4.0 km (Nuptse), 2.5 to 4.0 km (Lhotse Nup), 4.5 to 6.5 (Lhotse), and 1.5 to 2.5 km (Ama Dablam). Imja Glacier showed a small increase in ponded area between 1.0 and 1.5 km up-glacier. The two most recent images for Lhotse Shar

(Dec-13, Jan-15) revealed greatest pond expansion 2.0 to 4.5 km up-glacier, although ponded area in Dec-13 was higher than that of Jan-15.

5.2.2. Glacier-scale pond frequency

Increased hydrological connectivity is apparent in the lower 0.5 to 4 km of the Khumbu Glacier, which notably extends up the eastern margin (Fig. 7b). In this zone of high pond frequency (bounded by the black rectangle in Fig. 7b), ponded area increased by 33,593 m² (66%) (2009–2015). On the Khumbu Glacier, this connectivity between larger ponds was often by narrow inlets not easily identifiable on the imagery (Fig. 6a), but their existence was confirmed by field observations in Oct./Nov. 2015.

The smaller study glaciers (Fig. 7c) generally featured several distinct areas of high pond frequency (e.g. near the Nuptse terminus) but no evidence of increasing surface connectivity between pond basins. Lhotse Shar and Imja glaciers were an exception, where a large supraglacial lake (Imja Lake) is already established on the lower debris-covered area. Up-glacier of this lake there are discrete areas of high pond persistence along the full length of the debris-covered zone.

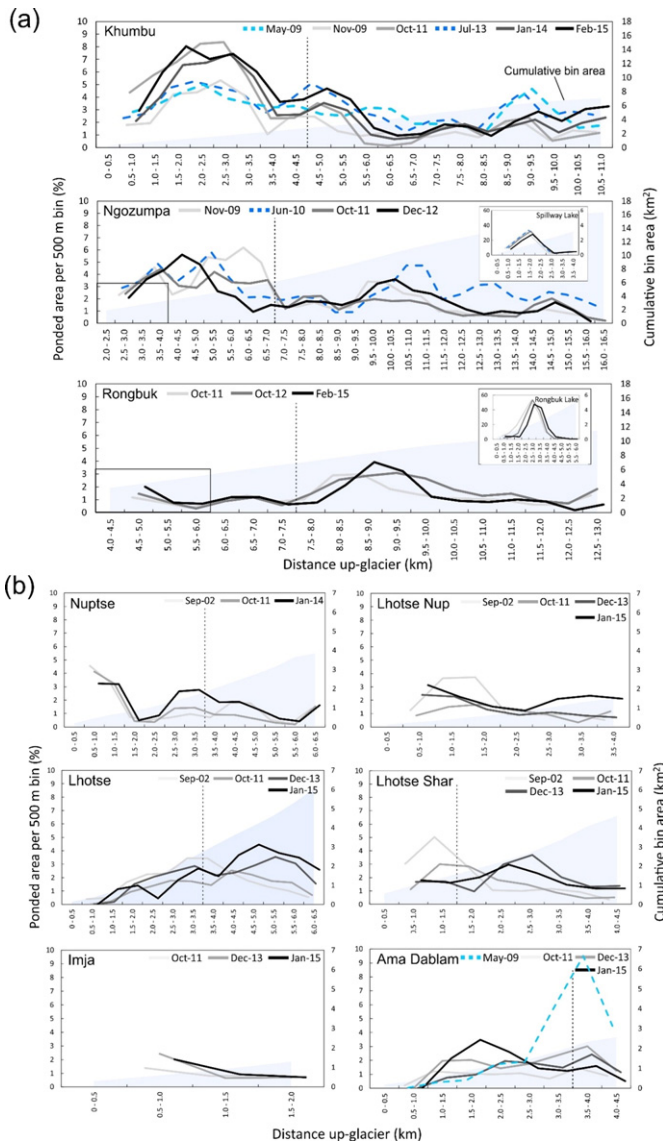


Fig. 5. Two-period moving average of ponded area with distance up-glacier, aggregated to 500 m bins. (a) The three largest study glaciers with Spillway and Rongbuk lakes shown inset for respective glaciers. (b) The smaller study glaciers. Vertical dashed line indicates the approximate transitions from active to inactive ice. This boundary is split on Lhotse Shar Glacier (see Fig. 7c).

Spillway and Rongbuk lakes persisted over our study period (Fig. 7a, d), although areas of drainage and growth were apparent at both locations (Fig. 6b, c). Drainage was especially pronounced on the lower terminus of the Rongbuk Glacier where a large pond drained over our study period (Nov-09–Dec-12) (Fig. 6c). On the Ngozumpa Glacier drainage events were widespread above Spillway Lake (Fig. 6b).

5.3. Cumulative pond area

Cumulative area distributions of supraglacial ponds revealed inter- and intra-annual variability across all of our study glaciers. Smaller ponds accounted for a proportionally greater area on summer images, relative to winter images (e.g. Fig. 8a, b, i). At a glacier scale, evidence of a recent trajectory towards smaller pond distributions was clear on several glaciers including Khumbu, Lhotse Nup, Lhotse, and Lhotse Shar (Fig. 8a, e–g).

The percentage of ponded area smaller than one (900 m^2) and four ($<3600 \text{ m}^2$) Landsat pixels was glacier dependent, reflecting contrasting pond-size distributions (Fig. 9a). A mean across all glaciers revealed

ponds $<900 \text{ m}^2$ accounted for 15 to 40% of total ponded area and those $<3600 \text{ m}^2$ accounted for 43 to 88%. When investigating the numbers of ponds, these statistics are notably higher at 77 to 89%, and 93 to 99% respectively (Fig. 9b). These statistics revealed potential omissions when using coarser-resolution (e.g. 30 m Landsat) imagery for supraglacial pond delineation. For a theoretical four-pixel ASTER imagery threshold (900 m^2), potential pond omissions for the larger glaciers in our study region (Khumbu, Ngozumpa, and Rongbuk) were in range of 17 to 19% of the overall ponded area (Fig. 9a). However, on smaller glaciers with smaller pond size distributions, this was up to 40% (Lhotse Nup Glacier). The vertical dashed lines on Fig. 8 provide a visual representation of potential omissions, which are variable by glacier, year, and season.

Our analysis revealed a trajectory towards large lake development for the Khumbu Glacier, with smaller ponds becoming more prevalent, in conjunction with an increase in the size of the largest pond observed, excluding Oct-11 (Fig. 8a). Spillway and Rongbuk lakes featured a stall in growth from historic trends (Ye et al., 2009; Thompson et al., 2012) and a decrease in overall area due to prominent drainage events.

6. Discussion

6.1. Trends in supraglacial pond development

Utilising an unprecedented spatiotemporal archive of fine-resolution satellite imagery, our results demonstrate a heterogeneous pattern of supraglacial pond and thus of temporary water storage dynamics in the Everest region glaciers.

Inter- and intra-annual pond change revealed in this study likely reflects a combination of meltwater generation (Gardelle et al., 2011), englacial inputs and drainages (Gulley and Benn, 2007), and precipitation inputs (Liu et al., 2015). Our detection of substantial year-to-year variations suggests that caution should be applied in studies using only a few images with a large temporal interval, since it is not known how representative a chosen image is over the respective timescale. Other studies have generally selected autumn and winter images for analysis of Himalayan glacier surfaces since low cloud cover often persists, and lake area changes are expected to be minimal at that time owing to negligible precipitation inputs (Gardelle et al., 2011; Thompson et al., 2012; Wang and Zhang, 2014; Liu et al., 2015). Our results demonstrated the magnitude of changes expected during the summer period for the Khumbu, Ngozumpa and Ama Dablam glaciers (Fig. 4). These summer dynamics have not previously been reported at a glacier-scale. The substantial summer pond growth we observed reveals the responsiveness of ponds to seasonal controls on precipitation and surface hydrology. The summer season features enhanced precipitation, pond ablation, meltwater generation, and increased pond connectivity with the englacial drainage system (Sakai et al., 2000; Wang et al., 2012; Miles et al., 2016). Pond development therefore proceeds alongside sporadic drainage events.

The area of supraglacial ponds is widely used as a proxy for their potential importance for water storage and glacier ablation (e.g. Gardelle et al., 2011; Liu et al., 2015; Wang et al., 2015; Zhang et al., 2015), however, volumetric estimates are required to assess true water storage dynamics. The compiled area-volume relationship dataset of Cook and Quincey (2015) features only two data points below a pond area of $10,000 \text{ m}^2$, hence pond bathymetry for the size of supraglacial ponds commonly encountered on our study glaciers is urgently required (Fig. 8). Nevertheless we present a first-order estimate of the volumetric contributions and temporal dynamics of supraglacial ponds for our study glaciers in Supplementary Table 2.

6.1.1. Glacier-scale ponded area patterns

Of the three largest glaciers, the Rongbuk featured a lower and less pronounced up-glacier ponded area distribution (Fig. 5a). We attribute this to an extensive supraglacial drainage stream, which extends the full

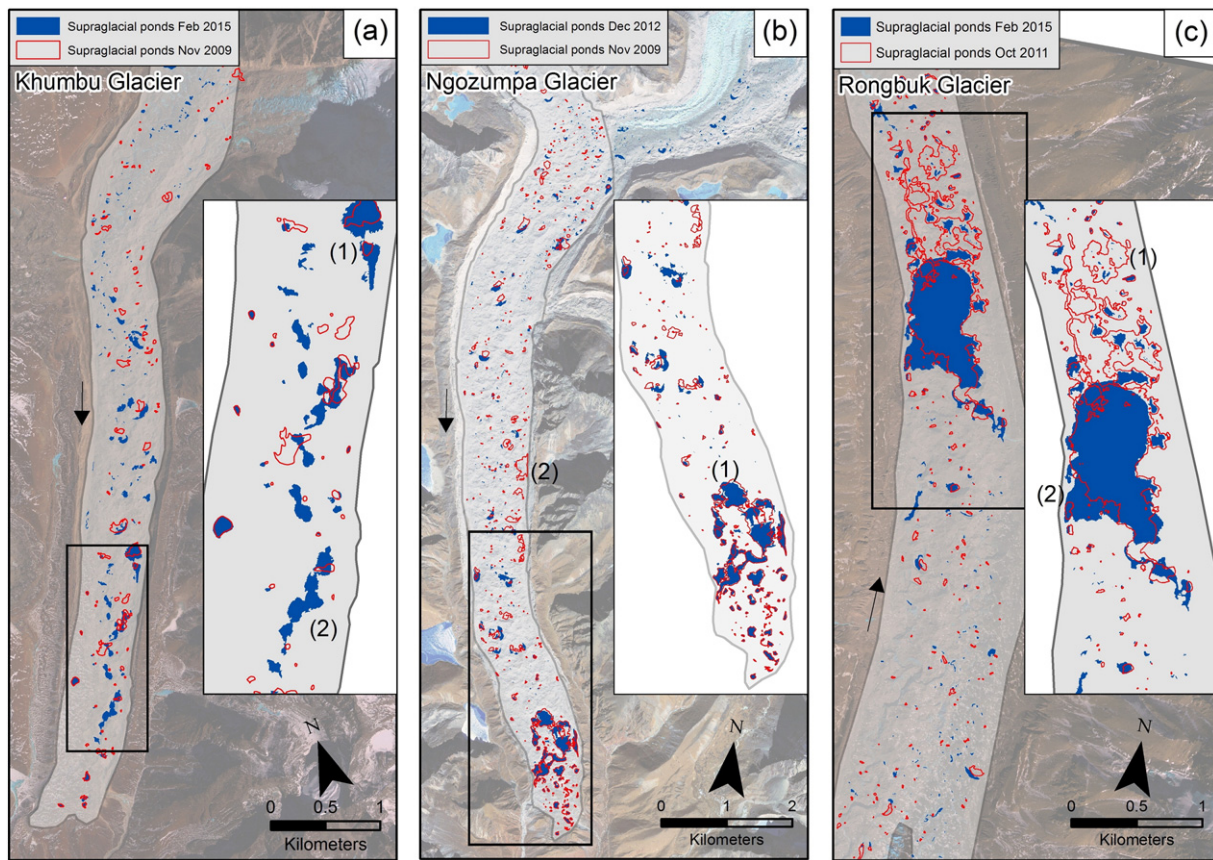


Fig. 6. Pondered area change for the Khumbu (a), Ngozumpa (b), and Rongbuk (c) glaciers, between the earliest and latest non-summer image. (a-1) Pond expansion, (a-2) pond expansion along the easterly margin, (b-1) up-glacier expansion and partial drainage of Spillway Lake, (b-2) mid-glacier pond drainage, (c-1) extensive drainage below Rongbuk Lake, and (c-2) up-glacier expansion of Rongbuk Lake. Arrows indicate ice flow direction. Satellite images courtesy of the DigitalGlobe Foundation.

length of the upper glacier before reaching Rongbuk Lake. The stream is likely able to efficiently drain a large proportion of meltwater generated from the extensive surface lowering identified by Ye et al. (2015). The active ice boundary approximated from Quincey et al. (2009) is also expected to have receded further up-glacier reflecting reduced glacier accumulation (Yang et al., 2006), allowing enhanced ponding in the 8 to 10 km zone (Fig. 5a). The Khumbu Glacier also features a supraglacial drainage network between 6 and 8 km up-glacier, which may explain the lower pond presence here, since repeated hydrofracturing in this area, which has compressional ice flow, allows supraglacial water drainage englacially (Benn et al., 2009). No extensive supraglacial drainage network exists on the Ngozumpa Glacier to explain similar zones of subdued ponded area. However, we note lower ponded area at ~13 km up-glacier, coinciding with the confluence of a tributary glacier (Figs. 5a and 6b).

Other factors contributing to ponded area dynamics exist: the prevalence of a low surface gradient ($<2^\circ$) across our study glaciers is well known (e.g. Quincey et al., 2007; Bolch et al., 2008a); similar debris-covered glaciers exhibit a non-linear mass-balance profile with elevation (Pellicciotti et al., 2015); and inactive ice is common across much or all of the debris-covered zones (e.g. Fig. 5 dashed vertical line), promoting pond expansion and coalescence (Bolch et al., 2008b; Quincey et al., 2009; Haritashya et al., 2015; Dehecq et al., 2015). Velocity fields created with fine-resolution imagery (e.g. Kraaijenbrink et al., 2016) have not yet been derived for glaciers in our study region, but would allow an association between glacier flow dynamics, surface lowering, and pond development, comparable to the imagery resolution used in this study. Internal pond feedbacks also act to enhance growth through the absorption and transmission of solar radiation to the

underlying ice (Sakai et al., 2000), and through ice cliff calving events at ponds of sufficient size (Sakai et al., 2009).

The Khumbu and Ngozumpa glaciers' (in particular the latter) featured repeat pond presence at similar locations through time (Figs. 5a and 7a, b). Glacier flow is expected to cause englacial conduit reorganisation and efficient drainage (Quincey et al., 2007), hence low pond frequencies would be expected in areas of active flow up-glacier, which supports our results. We did not conduct a pond-by-pond analysis in this study or an analysis of potential pond advection down glacier, although we expected this to be minimal over our study period. However, we suggest that the continued development of this fine-resolution dataset could reveal drainage and refill cycles of ponds at discrete locations, determined by glacier flow characteristics, and perhaps also influenced by basal topography of the glacier, similar to the topographic coupling observed on large ice sheets (e.g. Lampkin and VanderBerg, 2011). Within inactive ice zones, drainage events (e.g. Fig. 6b) reveal ponds are actively melting down at their base and intercepting englacial conduits or exploiting relic crevasse traces (Gulley and Benn, 2007). This is not apparent at Spillway and Rongbuk lakes, which have generally, although not entirely, displayed stability overall, with small areas of drainage and expansion. Spillway Lake is known to have a variable thickness of sediment on the lake bed, and contemporary expansion is concentrated around ice cliffs and regions of thin basal debris coverage (Thompson et al., 2012). The large drainage event down-glacier of Rongbuk Lake (Fig. 6c) was likely caused by interception with a supraglacial drainage channel close to the western pond margin.

Smaller glaciers in the region do not show a clear trend in the spatial distribution of ponded area, likely because although surface lowering is prevalent across the debris-covered zones, large ponds have not yet

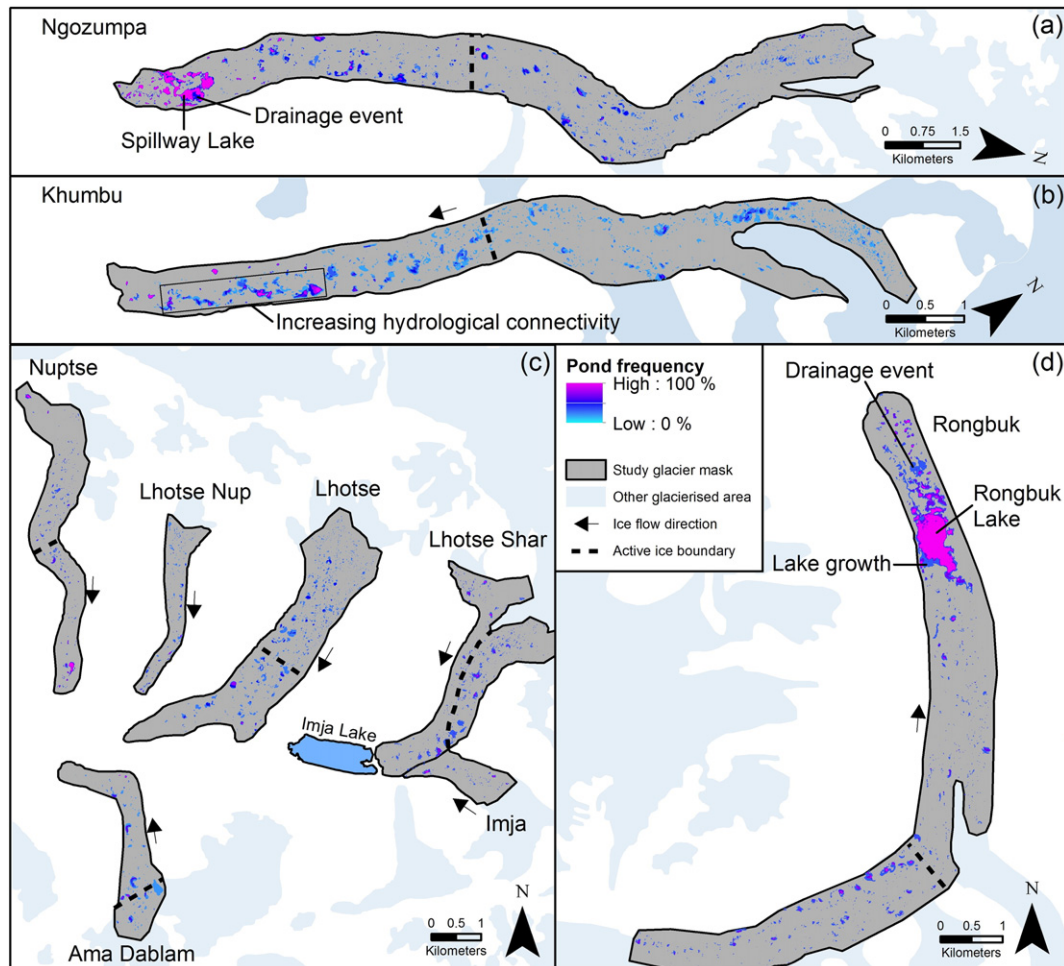


Fig. 7. Pond frequency normalised to the respective number of images used. Dashed lines indicate the approximate transition between active and inactive ice. A zoomed in view of Spillway and Rongbuk Lakes is shown in Supplementary Fig. 2 for clarity.

become established (Bolch et al., 2011) (Fig. 7c). However, a transitional trend towards smaller ponds is apparent (Fig. 5b), suggesting that smaller basins are becoming created and/or activated, concurrent with ongoing surface lowering. Potential overdeepenings in this region highlighted by Linsbauer et al. (2016) suggest that future glacial lakes could develop if supraglacial ponds begin to coalesce. Our results demonstrate a non-linear trend of ponded area increase in the region and an increasing importance of smaller ponds becoming established. Since our findings are expected to be applicable across Himalayan debris-covered glaciers in negative mass balance regimes, previously unreported smaller ponds will help understand the coupling between ponded area, local-scale topographic change, and a size-dependant influence of ponds on surface lowering.

6.1.2. Seasonal variation in supraglacial pond development

The temporal resolution available for several of our study glaciers revealed higher total ponded area during the summer season compared to preceding and succeeding winters (Fig. 4), and a transition towards smaller ponds accounting for proportionally greater area (Fig. 8). Increased thermal energy stored and transmitted by ponds to the underlying ice during the summer season increases meltwater generation and hence pond expansion (Sakai et al., 2000; Wang et al., 2012; Miles et al., 2016), in association with high precipitation during this season (Bookhagen and Burbank, 2006; Wagnon et al., 2013). The seasonal impact of this meltwater generation at a glacier-scale depends predominantly on the presence of outlets from ponds restricting expansion, and the role of sporadic drainage events transporting water englacially.

Our data suggest that ponds attain their maximum size during the summer period, increasing the likelihood of drainage through hydrofracture and the expansion of englacial conduits by warm pond water (Benn et al., 2009). Hence total ponded area is reduced approaching the winter period. The transition towards smaller ponds and a higher number of ponds during the summer season (Fig. 8, Table 3) suggests smaller basins become active, but exist as transient features, similarly draining approaching the winter period. Future studies tracking the development of individual ponds at similarly high temporal and spatial resolution, coupled with pond-scale energy balance modelling (e.g. Miles et al., 2016) is required to refine understanding of debris-covered glacier surface hydrology and the importance for ablation at a glacier-scale.

6.2. Lake development trajectory

The development of large glacial lakes in the region raises concerns about future GLOF risk (Benn et al., 2012), and rapid glacier mass loss and glacier retreat if a calving front develops (e.g. Imja Lake) (Somos-Valenzuela et al., 2014). Recent expansion of supraglacial ponds on the eastern margin of the Khumbu Glacier (Figs. 6a and 7b) suggests it may be entering a transitional phase towards large glacial lake development in the lower ablation area. This development was proposed by Naito's et al. (2000) modelling study, and a large overdeepened basin on the lower ablation area was modelled by Linsbauer et al. (2016). We identified a winter image trajectory towards smaller ponds contributing greater total ponded area (Fig. 5a), larger ponds overall (Fig. 8a),

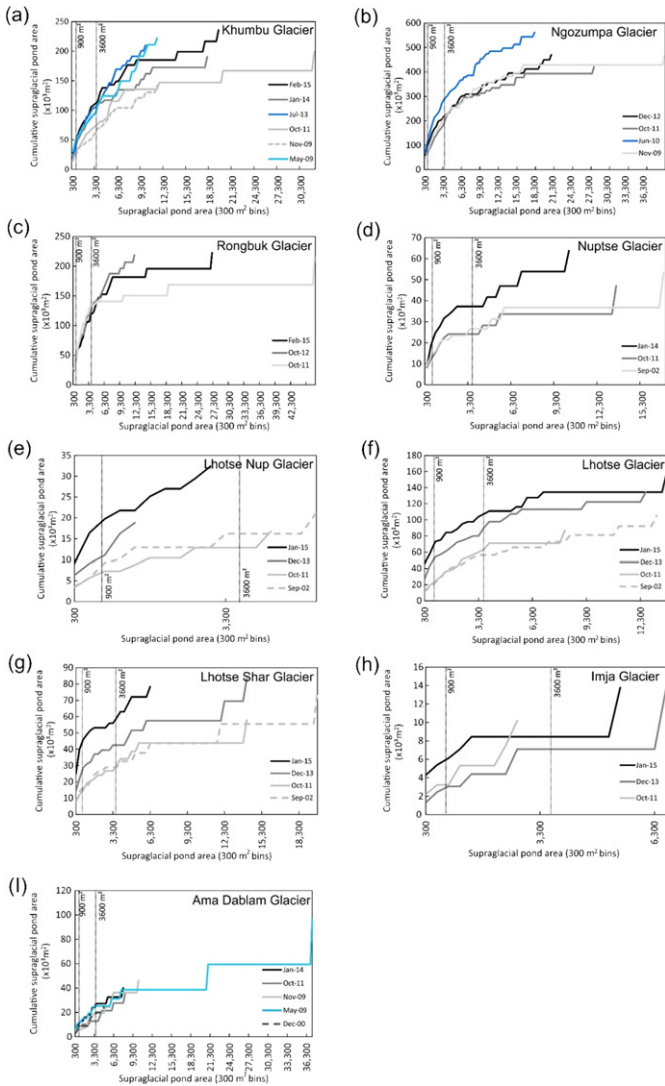


Fig. 8. Cumulative pond area distribution for post-monsoon/Winter (PMW) images (grey scale) and pre-monsoon/monsoon (PMM) (blue scale) time periods. The terminal lakes on the Ngozumpa and Rongbuk glaciers are not shown here for clarity.

and an increase in ponded area in the lower ablation zone of the Khumbu Glacier (Fig. 5a). This pattern suggests firstly that small basins are becoming occupied with meltwater as surface lowering prevails, promoting the development of a reverse glacier surface gradient (Bolch et al., 2011), and secondly that these ponds are now persisting in some cases and coalescing into a connected chain of ponds. The outlet pond on the Khumbu Glacier represents the hydrological base level at the eastern lateral moraine, and was observed in the field and on satellite imagery to have high sediment build up on the bed. This sedimentation and subsequent insulation of any remaining ice below promotes a stable base level, which is conducive to the connection and expansion of ponds up-glacier, following trends of Imja, Spillway, and Rongbuk lakes. However, in the case of the Khumbu Glacier, across-glacier expansion is restricted by a vegetated stable zone to the west.

Thompson et al. (2012) revealed an exponential growth rate of Spillway Lake since 2001, from lake inception in the 1980s. Rongbuk Lake began development 1990s but has shown similar rapid expansion (Chen et al., 2014). However, in our study, both lakes decreased in area (Spillway Lake: net loss of 8345 m² Nov-09 to Jun-15, Rongbuk lake: net loss of 87,451 m² Oct-11 to Feb-15) despite expanding up-glacier (Fig. 5a insets). We propose that although these lakes are continuing to expand up-glacier through ice cliff retreat and basal melt, they have stalled due to supraglacial drainage channel evolution and a likely lowering of the hydrological base level. Thompson et al. (2012) identified that a connection made between 2001 and 2009 between Spillway Lake and a second smaller lake closer to an easterly draining supraglacial channel, had the potential to re-route the drainage of Spillway Lake and lower the hydrological base level, causing a likely stall in the lake expansion. However, our Dec-2012 image revealed that this channel did not develop and that drainage is still predominantly through the western moraine. If this western channel incised and subsequently lowered the base level, this could explain the lake drainage observed in this study as the lake level adjusts (e.g. Fig. 6b). Contemporary expansion to Jun-15 (Table 3) suggests this channel has now stabilised and up-glacier expansion of Spillway Lake is likely to continue.

6.3. Uncertainties in pond detection and delineation

Previous studies reporting supra- and pro-glacial lake dynamics in the Everest region have utilised the long temporal archive of Landsat imagery (e.g. Gardelle et al., 2011; Nie et al., 2013; Bhardwaj et al., 2015; Liu et al., 2015; Wang et al., 2015). Landsat features a relatively short revisit period (16 days), hence cloud free images are usually

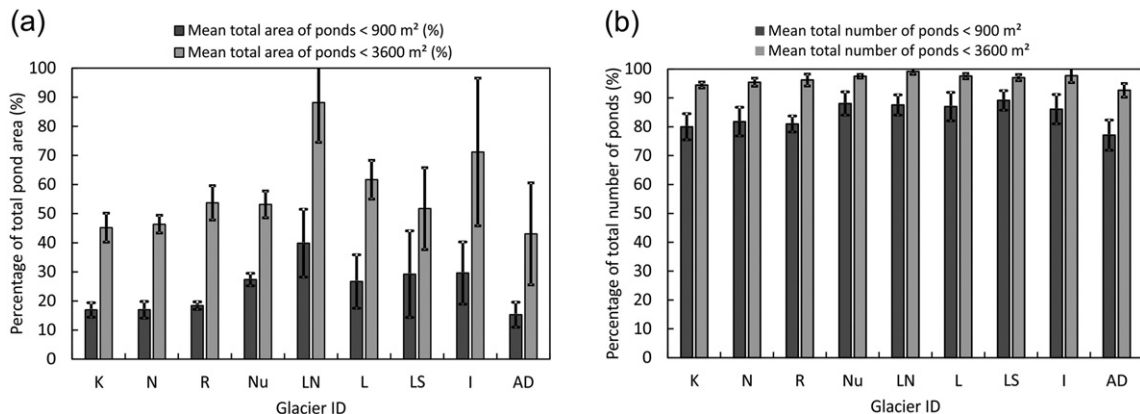


Fig. 9. Proportion of (a) pond areas and (b) pond frequency, falling below a 900 m²/3600 m² threshold for each study glacier. Values represent a mean across all time periods and error bars show standard deviation.

available outside of the monsoon season. Other multi-temporal studies have used a range of fine-to-coarse resolution imagery, often in combination (Table 1).

Decadal trends across the Himalaya were presented by Gardelle et al. (2011) and Nie et al. (2013) using Landsat imagery from three and four time periods, using a four and nine 30 m pixel minimum detection threshold, respectively. Whilst our results are broadly in agreement with observed increasing water storage trends in the Everest region, we highlight notable short-term variability and suggest that Landsat imagery is not appropriate for glacier-scale pond monitoring in the Himalaya.

The irregular shape (mean circularity index values of 1.4 to 3.5, Table 3) and size distribution of ponds (Figs. 2 and 8) does not lend to alignment with a 30 m pixel (Fig. 10), since a large proportion of ponded area is accounted for by small ponds. Firstly, this suggests that approximating ponds as circular objects for purposes of uncertainty estimation is not appropriate, since pond circularity is highly variable but rarely approaching the ideal value of one (Table 3). Secondly, this study revealed that ponds <900 m² accounted for 15 to 40% of total ponded area and those <3600 m² accounted for 43 to 88% (Fig. 9). When quantifying the numbers of ponds present, these statistics were 77 to 89% and 93 to 99% respectively. Although the total number of ponds is less important than overall area, the distribution of smaller ponds indicates where debris-cover is likely to be thin, and so integration with energy balance models and surface lowering maps would be beneficial. These statistics represent potential pond omissions using thresholds of 900 m² and 3600 m², which represent the area of four ASTER pixels (15 m) or one Landsat pixel (30 m), and four Landsat pixels respectively. Since the application of this imagery usually relies on a variable NDWI threshold, our error estimates represent the upper bounds. Nonetheless, a broad threshold is often used to capture mixed pixels containing majority water (e.g. Gardelle et al., 2011), hence ponded area could equally be systematically overestimated if pond distributions tend towards smaller ponds on the order of one 30 m pixel (Fig. 10c). We show an idealised theoretical variation in ponded area with variable threshold in Supplementary Fig. 3.

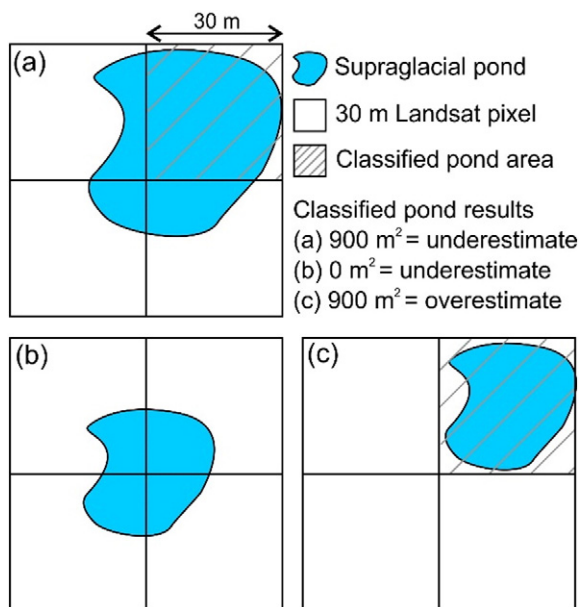


Fig. 10. Hypothetical pond classification scenarios using Landsat imagery. Classifications are dependent on a user-determined threshold which assigns ponds to a raster grid based on the strength of their spectral signature within each pixel. (a) The pond is larger than one pixel but covers a small proportion of three adjacent pixels, (b) The pond is aligned at the centre of four pixels but does not dominate any, and (c) the pond is smaller than one pixel but dominates the spectral signature and is classified as one pixel in size.

This study has also shown that pond size-area distributions are not static (Fig. 8), hence revealing the potential for an inter-annual and seasonal bias when using multi-temporal Landsat images for supraglacial pond delineation. The small size and shallow nature of supraglacial ponds (Cook and Quincey, 2015) means area fluctuations can be large, which requires a small pixel size (<10 m) for adequate detection of seasonal trends (Strozzi et al., 2012). Supraglacial pond delineation with coarser resolution imagery is also hindered by pond turbidity and frozen ponds (Bhatt et al., 2007; Racoviteanu et al., 2008). On the Khumbu Glacier we observed a large number of frozen or partially frozen surfaces upon commencement of a field campaign (11th Oct 2015). For this reason, we suggest a transition towards finer-resolution imagery is advantageous for multi-temporal monitoring of supraglacial ponds. However, we acknowledge that Landsat imagery will continue to be a valuable asset when monitoring larger glacial lakes where the edge effects of pixel resolution are substantially lower.

7. Conclusion and future work

This study presents the first extensive application of fine-resolution satellite imagery to undertake a multi-temporal, multi-glacier analysis of supraglacial pond dynamics. Inter- and intra-annual changes in glacier-scale ponded area were up to 17% and 52% respectively, reflecting drainage events, pond expansion and coalescence, and melt season pond expansion. Additionally, despite the prevalence of a negative mass balance regime, a net increase in ponded area was only apparent on six of our nine study glaciers. This short-term variability may sit within decadal scale regional increases (e.g. Gardelle et al., 2011), but nevertheless indicates that stagnating, low gradient, and thinning debris-covered glaciers in the Himalaya do not linearly accrue ponded area through time without notable inter- and intra-annual variability. An evolutionary trajectory towards smaller ponds accounting for larger proportional area was discovered for several glaciers including: Khumbu, Nuptse, Lhotse Nup, Lhotse, and Lhotse Shar. Therefore, pond size distribution appears intrinsically linked to the evolution of debris-covered glaciers under negative mass balance and is likely to have consequent implications for the positive-feedback enhancement of melt, in and around the pond environment (Sakai et al., 2000).

Spillway and Rongbuk lakes, previously thought to be expanding exponentially, featured a halt in growth during our study period due to notable drainage events. These drainages were likely caused by (i) lowering of the hydrological base level, and (ii) interception with a supraglacial drainage network, respectively. However, both lakes are actively growing up-glacier and so will likely continue to expand once supraglacial drainage channels have stabilised, as evidenced for the Ngozumpa Glacier. The formation and persistence of a chain of ponds on the lower ablation area of the Khumbu Glacier is indicative of a transitional phase towards large lake development in association with a stable hydrological base level, and should be monitored over coming years.

We have shown that fine-resolution imagery is necessary to represent the full spectrum of supraglacial pond sizes that exist on debris-covered glaciers in the Everest region of the central Himalaya. Medium-resolution imagery (e.g. 30 m Landsat) is likely to lead to large omissions of supraglacial water storage on the order of 15 to 88% of total ponded area, and 77 to 99% of the total number of ponds. Nonetheless, medium-resolution Landsat imagery will remain valuable for large glacial lake monitoring, but small changes in water level (e.g. inter-annual) are likely to be missed (Strozzi et al., 2012). Inter-annual and seasonal biases would also be expected when using medium-resolution satellite imagery, since cumulative pond-size distributions were found to vary inter- and intra-annually, and were glacier specific.

Acknowledgements

The DigitalGlobe Foundation is thanked for access to satellite imagery, which made this study possible. C.S.W acknowledges fieldwork

support from the School of Geography at the University of Leeds, the Royal Geographical Society (with IBG), the British Society for Geomorphology, and water@leeds. Dhananjay Regmi and our logistics team from Himalayan Research Expeditions are thanked for invaluable support during fieldwork, Pascal Buri for loan of a boat, and the NERC Geophysical Equipment Facility for loan of a dGPS and technical assistance. We thank the reviewers of an earlier manuscript for constructive comments.

Appendix A. Supplementary data

Supplementary data to this article can be found online at <http://dx.doi.org/10.1016/j.gloplacha.2016.04.008>.

References

- Benn, D.I., Bolch, T., Hands, K., Gulley, J., Luckman, A., Nicholson, L.L., Quincey, D., Thompson, S., Toumi, R., Wiseman, S., 2012. Response of debris-covered glaciers in the Mount Everest region to recent warming, and implications for outburst flood hazards. *Earth-Sci. Rev.* 114 (1–2), 156–174.
- Benn, D., Gulley, J., Luckman, A., Adamek, A., Glowacki, P.S., 2009. Englacial drainage systems formed by hydrologically driven crevasse propagation. *J. Glaciol.* 55 (191), 513–523.
- Benn, D.I., Wiseman, S., Hands, K.A., 2001. Growth and drainage of supraglacial lakes on debris-mantled Ngozumpa Glacier, Khumbu Himal, Nepal. *J. Glaciol.* 47 (159), 626–638.
- Bhardwaj, A., Singh, M.K., Joshi, P.K., Snehan Singh, S., Sam, L., Gupta, R.D., Kumar, R., 2015. A lake detection algorithm (LDA) using Landsat 8 data: a comparative approach in glacial environment. *Int. J. Appl. Earth Obs. Geoinf.* 38, 150–163.
- Bhatt, M.P., Masuzawa, T., Yamamoto, M., Takeuchi, N., 2007. Chemical characteristics of pond waters within the debris area of Lirung Glacier in Nepal Himalaya. *J. Limnol.* 66, 71–80.
- Bolch, T., Buchroithner, M.F., Peters, J., Baessler, M., Bajracharya, S., 2008b. Identification of glacier motion and potentially dangerous glacial lakes in the Mt. Everest region/Nepal using spaceborne imagery. *Nat. Hazards Earth Syst. Sci.* 8 (6), 1329–1340.
- Bolch, T., Buchroithner, M., Pieczonka, T., Kunert, A., 2008a. Planimetric and volumetric glacier changes in the Khumbu Himal, Nepal, since 1962 using Corona, Landsat TM and ASTER data. *J. Glaciol.* 54 (187), 592–600.
- Bolch, T., Pieczonka, T., Benn, D.I., 2011. Multi-decadal mass loss of glaciers in the Everest area (Nepal Himalaya) derived from stereo imagery. *Cryosphere* 5 (2), 349–358.
- Bookhagen, B., Burbank, D.W., 2006. Topography, relief, and TRMM-derived rainfall variations along the Himalaya. *Geophys. Res. Lett.* 33 (8), 1–5.
- Carrivick, J.L., Tweed, F.S., 2013. Proglacial lakes: character, behaviour and geological importance. *Quat. Sci. Rev.* 78, 34–52.
- Chen, W., Doko, T., Liu, C., Ichinose, T., Fukui, H., Feng, Q., Gou, P., 2014. Changes in Rongbuk lake and Imja Lake in the Everest region of Himalaya. *Int. Arch. Photogramm. Remote. Sens. Spat. Inf. Sci.* 259–266.
- Cook, S.J., Quincey, D.J., 2015. Estimating the volume of Alpine glacial lakes. *Earth Surf. Dynam.* 3, 559–575.
- Dehecq, A., Gourmelen, N., Trouve, E., 2015. Deriving large-scale glacier velocities from a complete satellite archive: application to the Pamir–Karakoram–Himalaya. *Remote Sens. Environ.* 162, 55–66.
- Gardelle, J., Arnaud, Y., Berthier, E., 2011. Contrasted evolution of glacial lakes along the Hindu Kush Himalaya mountain range between 1990 and 2009. *Glob. Planet. Chang.* 75 (1–2), 47–55.
- Gulley, J., Benn, D.I., 2007. Structural control of englacial drainage systems in Himalayan debris-covered glaciers. *J. Glaciol.* 53 (182), 399–412.
- Haritashya, U.K., Pleasants, M.S., Copland, L., 2015. Assessment of the evolution in velocity of two debris-covered glaciers in Nepal and New Zealand. *Geogr. Ann. A Phys. Geogr.* 97 (4), 737–751.
- Immerzeel, W.W., Kraaijenbrink, P.D.A., Shea, J.M., Shrestha, A.B., Pellicciotti, F., Bierkens, M.F.P., de Jong, S.M., 2014. High-resolution monitoring of Himalayan glacier dynamics using unmanned aerial vehicles. *Remote Sens. Environ.* 150, 93–103.
- Inoue, J., Yoshida, M., 1980. Ablation and heat exchange over the khumbu glacier. *J. Jpn. Soc. Snow Ice (Seppyo)* 39, 7–14.
- Iwata, S., Aoki, T., Kadiota, T., Seko, K., Yamaguchi, S., 2000. Morphological evolution of the debris cover on Khumbu Glacier, Nepal, between 1978 and 1995. In: Nakawo, M., Raymond, C.F., Fountain, A. (Eds.), *IAHS Publ. 264 (Symposium at Seattle 2000 – Debris-Covered Glaciers)*, Seattle, Washington, U.S.A. IAHS Publication, pp. 3–12.
- Kääb, A., Berthier, E., Nuth, C., Gardelle, J., Arnaud, Y., 2012. Contrasting patterns of early twenty-first-century glacier mass change in the Himalayas. *Nature* 488 (7412), 495–498.
- Komori, J., 2008. Recent expansions of glacial lakes in the Bhutan Himalayas. *Quat. Int.* 184 (1), 177–186.
- Kraaijenbrink, P., Meijer, S.W., Shea, J.M., Pellicciotti, F., de Jong, S.M., Immerzeel, W.W., 2016. Seasonal surface velocities of a Himalayan glacier derived by automated correlation of unmanned aerial vehicle imagery. *Ann. Glaciol.* 57 (71), 103–113.
- Lampkin, D.J., VanderBerg, J., 2011. A preliminary investigation of the influence of basal and surface topography on supraglacial lake distribution near Jakobshavn Isbrae, western Greenland. *Hydrol. Process.* 25 (21), 3347–3355.
- Linsbauer, A., Frey, H., Haeblerli, W., Machguth, H., Azam, M.F., Allen, S., 2016. Modelling glacier-bed overdeepenings and possible future lakes for the glaciers in the Himalaya–Karakoram. *Ann. Glaciol.* 57 (71).
- Liu, D., Xia, F., 2010. Assessing object-based classification: advantages and limitations. *Remote Sens. Lett.* 1 (4), 187–194.
- Liu, Q., Christoph, M., Shiyin, L., 2015. Distribution and interannual variability of supraglacial lakes on debris-covered glaciers in the Khan Tengri-Tumor Mountains, Central Asia. *Environ. Res. Lett.* 10 (1), 1–10.
- Miles, E.S., Pellicciotti, F., Willis, I.C., Steiner, J.F., Buri, P., Arnold, N.S., 2016. Refined energy-balance modelling of a supraglacial pond, Langtang Khola, Nepal. *Ann. Glaciol.* 57 (71), 29–40.
- Mölg, T., Maussion, F., Yang, W., Scherer, D., 2012. The footprint of Asian monsoon dynamics in the mass and energy balance of a Tibetan glacier. *Cryosphere* 6 (6), 1445–1461.
- Naito, N., Nakawo, M., Kadota, T., Raymond, C.F., 2000. Numerical simulation of recent shrinkage of Khumbu Glacier, Nepal Himalayas. In: Nakawo, M., Raymond, C.F., Fountain, A. (Eds.), *IAHS Publ. 264 (Symposium at Seattle 2000 – Debris-Covered Glaciers)*, Seattle, Washington, U.S.A. IAHS Publication, pp. 245–254.
- Nakawo, M., Iwata, S., Watanabe, O., Yoshida, M., 1986. Processes which distribute supraglacial debris on the Khumbu Glacier, Nepal Himalaya. *Ann. Glaciol.* 8, 129–131.
- Nie, Y., Liu, Q., Liu, S., 2013. Glacial lake expansion in the central Himalayas by Landsat images, 1990–2010. *PLoS One* 8 (12), 1–8.
- Nie, Y., Zhang, Y.L., Liu, L.S., Zhang, J.P., 2010. Glacial change in the vicinity of Mt. Qomolangma (Everest), central high Himalayas since 1976. *J. Geogr. Sci.* 20 (5), 667–686.
- Pellicciotti, F., Stephan, C., Miles, E., Herreid, S., Immerzeel, W.W., Bolch, T., 2015. Mass-balance changes of the debris-covered glaciers in the Langtang Himal, Nepal, from 1974 to 1999. *J. Glaciol.* 61 (226), 373–386.
- Pfeffer, W.T., Arendt, A.A., Bliss, A., Bolch, T., Cogley, J.G., Gardner, A.S., Hagen, J.O., Hock, R., Kaser, G., Kienholz, C., Miles, E.S., Moholdt, G., Mölg, N., Paul, F., Radic, V., Rastner, P., Raup, B.H., Rich, J., Sharp, M.J., Randolph, C., 2014. The Randolph glacier inventory: a globally complete inventory of glaciers. *J. Glaciol.* 60 (221), 537–552.
- Quincey, D.J., Luckman, A., Benn, D., 2009. Quantification of Everest region glacier velocities between 1992 and 2002, using satellite radar interferometry and feature tracking. *J. Glaciol.* 55 (192), 596–606.
- Quincey, D.J., Richardson, S.D., Luckman, A., Lucas, R.M., Reynolds, J.M., Hambrey, M.J. and Glasser, N.F. 2007. Early recognition of glacial lake hazards in the Himalaya using remote sensing datasets. *Glob. Planet. Chang.* 56(1–2), 137–152.
- Racoviteanu, A.E., Williams, M.W., Barry, R.G., 2008. Optical remote sensing of glacier characteristics: a review with focus on the Himalaya. *Sensors* 8 (5), 3355–3383.
- Reid, T.D., Brock, B.W., 2014. Assessing ice-cliff backwasting and its contribution to total ablation of debris-covered Miage glacier, Mont Blanc massif, Italy. *J. Glaciol.* 60 (219), 3–13.
- Richardson, S.D., Reynolds, J.M., 2000. An overview of glacial hazards in the Himalayas. *Quat. Int.* 65–66, 31–47.
- Rohl, K., 2006. Thermo-erosional notch development at fresh-water-calving Tasman Glacier, New Zealand. *J. Glaciol.* 52 (177), 203–213.
- Rohl, K., 2008. Characteristics and evolution of supraglacial ponds on debris-covered Tasman Glacier, New Zealand. *J. Glaciol.* 54 (188), 867–880.
- Rowan, A.V., Egholm, D.L., Quincey, D.J., Glasser, N.F., 2015. Modelling the feedbacks between mass balance, ice flow and debris transport to predict the response to climate change of debris-covered glaciers in the Himalaya. *Earth Planet. Sci. Lett.* 430, 427–438.
- Sakai, A., Nishimura, K., Kadota, T., Takeuchi, N., 2009. Onset of calving at supraglacial lakes on debris-covered glaciers of the Nepal Himalaya. *J. Glaciol.* 55 (193), 909–917.
- Sakai, A., Takeuchi, N., Fujita, K., Nakawo, M., 2000. Role of supraglacial ponds in the ablation process of a debris-covered glacier in the Nepal Himalayas. In: Nakawo, M., Raymond, C.F., Fountain, A. (Eds.), *IAHS Publ. 264 (Symposium at Seattle 2000 – Debris-Covered Glaciers)*, Seattle, Washington, U.S.A. IAHS Publishing, pp. 119–130.
- Salerno, F., Guyennon, N., Thakuri, S., Viviano, G., Romano, E., Vuillermoz, E., Cristofanelli, P., Stocchi, P., Agrillo, G., Ma, Y., Tartari, G., 2015. Weak precipitation, warm winters and springs impact glaciers of south slopes of Mt. Everest (central Himalaya) in the last 2 decades (1994–2013). *Cryosphere* 9 (3), 1229–1247.
- Salerno, F., Thakuri, S., D'Agata, C., Smiraglia, C., Manfredi, E.C., Viviano, G., Tartari, G., 2012. Glacial lake distribution in the Mount Everest region: uncertainty of measurement and conditions of formation. *Glob. Planet. Chang.* 92–93, 30–39.
- Shrestha, A.B., Aryal, R., 2011. Climate change in Nepal and its impact on Himalayan glaciers. *Reg. Environ. Chang.* 11, 65–77.
- Somos-Valenzuela, M.A., McKinney, D.C., Rounce, D.R., Byers, A.C., 2014. Changes in Imja Tsho in the Mount Everest region of Nepal. *Cryosphere* 8 (5), 1661–1671.
- Steiner, J.F., Pellicciotti, F., Buri, P., Miles, E.S., Immerzeel, W.W., Reid, T.D., 2015. Modelling ice-cliff backwasting on a debris-covered glacier in the Nepalese Himalaya. *J. Glaciol.* 61 (229), 889–907.
- Strozzi, T., Wiesmann, A., Kaab, A., Joshi, S., Mool, P., 2012. Glacial lake mapping with very high resolution satellite SAR data. *Nat. Hazards Earth Syst. Sci.* 12 (8), 2487–2498.
- Thompson, S.S., Benn, D.I., Dennis, K., Luckman, A., 2012. A rapidly growing moraine-dammed glacial lake on Ngozumpa Glacier, Nepal. *Geomorphology* 145, 1–11.
- Veettil, B., Bianchini, N., de Andrade, A., Bremer, U., Simões, J., de Souza Junior, E., 2015. Glacier changes and related glacial lake expansion in the Bhutan Himalaya, 1990–2010. *Reg. Environ. Chang.* 1–12.
- Wagnon, P., Vincent, C., Arnaud, Y., Berthier, E., Vuillermoz, E., Gruber, S., Ménégoz, M., Gilbert, A., Dumont, M., Shea, J.M., Stumm, D., Pokhrel, B.K., 2013. Seasonal and annual mass balances of Mera and Pokalde glaciers (Nepal Himalaya) since 2007. *Cryosphere* 7 (6), 1769–1786.
- Wang, S., Zhang, T., 2014. Spatial change detection of glacial lakes in the Koshi River Basin, the central Himalayas. *Environ. Earth Sci.* 72 (11), 4381–4391.

- Wang, X., Liu, S.Y., Han, H.D., Wang, J., Liu, Q., 2012. Thermal regime of a supraglacial lake on the debris-covered Koxkar Glacier, southwest Tianshan, China. *Environ. Earth Sci.* 67 (1), 175–183.
- Wang, W.C., Xiang, Y., Gao, Y., Lu, A.X., Yao, T.D., 2015. Rapid expansion of glacial lakes caused by climate and glacier retreat in the central Himalayas. *Hydrol. Process.* 29 (6), 859–874.
- Watanabe, T., Ives, J.D., Hammond, J.E., 1994. Rapid growth of a glacial lake in Khumbu Himal, Himalaya: prospects for a catastrophic flood. *Mt. Res. Dev.* 14 (4), 329–340.
- Wessels, R.L., Kargel, J.S., Kieffer, H.H., 2002. ASTER measurement of supraglacial lakes in the Mount Everest region of the Himalaya. *Ann. Glaciol.* 34, 399–408.
- Yang, X., Zhang, Y., Zhang, W., Yan, Y., Wang, Z., Ding, M., Chu, D., 2006. Climate change in Mt. Qomolangma region since 1971. *J. Geogr. Sci.* 16 (3), 326–336.
- Ye, Q., Bolch, T., Naruse, R., Wang, Y., Zong, J., Wang, Z., Zhao, R., Yang, D., Kang, S., 2015. Glacier mass changes in Rongbuk catchment on Mt. Qomolangma from 1974 to 2006 based on topographic maps and ALOS PRISM data. *J. Hydrol.* 530, 273–280.
- Ye, Q., Zhong, Z., Kang, S., Stein, A., Wei, Q., Liu, J., 2009. Monitoring glacier and supraglacial lakes from space in Mt. Qomolangma region of the Himalayas on the Tibetan Plateau in China. *J. Mt. Sci.* 6 (3), 211–220.
- Zhang, G., Yao, T., Xie, H., Wang, W., Yang, W., 2015. An inventory of glacial lakes in the Third Pole region and their changes in response to global warming. *Glob. Planet. Chang.* 131, 148–157.